Detailed Kinetic Analysis of a Family 52 Glycoside Hydrolase: A β-Xylosidase from Geobacillus stearothermophilus †

ARTICLE *in* BIOCHEMISTRY · SEPTEMBER 2003

Impact Factor: 3.02 · DOI: 10.1021/bi034505o · Source: PubMed

7 AUTHORS, INCLUDING:

Valery Belakhov
Technion - Israel Institute of Technology
97 PUBLICATIONS **1,404** CITATIONS
SEE PROFILE

Yuval Shoham
Technion - Israel Institute of Technology
175 PUBLICATIONS **6,674** CITATIONS
SEE PROFILE

Detailed Kinetic Analysis of a Family 52 Glycoside Hydrolase: A β-Xylosidase from *Geobacillus stearothermophilus*†

Tsafrir Bravman,‡ Gennady Zolotnitsky,‡ Valery Belakhov,§ Gil Shoham,|| Bernard Henrissat,⊥ Timor Baasov,*,§,# and Yuval Shoham*,‡,#

Department of Food Engineering and Biotechnology, Department of Chemistry, and Institute of Catalysis Science and Technology, Technion-Israel Institute of Technology, Haifa 32000, Israel, Department of Inorganic Chemistry and The Laboratory for Structural Chemistry and Biology, The Hebrew University of Jerusalem, Jerusalem 91904, Israel, and Architecture et Fonction des Macromolécules Biologiques, UMR6098, CNRS, and Universités d'Aix-Marseille I and II, 31 Chemin Joseph Aiguier, 13402 Marseille Cedex 20, France

Received March 31, 2003; Revised Manuscript Received July 7, 2003

ABSTRACT: *Geobacillus stearothermophilus* T-6 encodes for a β-xylosidase (XynB2) from family 52 of glycoside hydrolases that was previously shown to hydrolyze its substrate with net retention of the anomeric configuration. XynB2 significantly prefers substrates with xylose as the glycone moiety and exhibits a typical bell-shaped pH dependence curve. Binding properties of xylobiose and xylotriose to the active site were measured using isothermal titration calorimetry (ITC). Binding reactions were enthalpy driven with xylobiose binding more tightly than xylotriose to the active site. The kinetic constants of XynB2 were measured for the hydrolysis of a variety of aryl β-D-xylopyranoside substrates bearing different leaving groups. The Brønsted plot of log k_{cat} versus the pK_a value of the aglycon leaving group reveals a biphasic relationship, consistent with a double-displacement mechanism as expected for retaining glycoside hydrolases. Hydrolysis rates for substrates with poor leaving groups (pK_a > 8) vary widely with the aglycon reactivity, indicating that, for these substrates, the bond cleavage is rate limiting. However, no such dependence is observed for more reactive substrates (pK_a < 8), indicating that in this case hydrolysis of the xylosyl-enzyme intermediate is rate limiting. Secondary kinetic isotope effects suggest that the intermediate breakdown proceeds with modest oxocarbenium ion character at the transition state, and bond cleavage proceeds with even lower oxocarbenium ion character. Inhibition studies with several gluco analogue inhibitors could be measured since XynB2 has low, yet sufficient, activity toward 4-nitrophenyl β-D-glucopyranose. As expected, inhibitors mimicking the proposed transition state structure, such as 1-deoxynojirimycin, bind with much higher affinity to XynB2 than ground state inhibitors.

Xylan is the major hemicellulosic polysaccharide in the plant cell wall representing up to 30%−35% of the total dry mass. This polymer is composed of a β-1,4-linked xylopyranosyl backbone substituted with different side chains such as arabinofuranose, methylglucuronic acid, and acetyl. Because of its structural complexity, complete degradation of xylan requires synergistic action of several hemicellulolytic enzymes (*1*). Among others, these include endo-1,4-β-xylanases (EC 3.2.1.8), which hydrolyze the xylan backbone, and β-D-xylosidases (EC 3.2.1.37), which cleave the resulting xylooligomers to free xylose. Hemicellulases are vital for maintaining the carbon cycle in nature, since they are responsible for the complete degradation of the plant biomass to soluble saccharides. These in turn are utilized as carbon or energy sources for microorganisms and higher animals. Hemicellulases gained much attention because of their capability to reduce costs and environmental impact in various biotechnological applications such as biobleaching in the paper and pulp industry (*1*, *2*), the degradation of lignocellulosic material for the production of bioethanol (*3*, *4*), and recently in the field of oligosaccharide and thioglycoside synthesis (*5*, *6*).

Glycoside hydrolases cleave the glycosidic bond, which is one of the most stable bonds within all biopolymers in nature with a half-life of over 5 millions years (*7*). These

† This work was supported in part by The Israel Science Foundation (Grant 676/00 to G.S. and Y.S.) and by the French−Israeli Association for Scientific and Technological Research (AFIRST, to B.H and Y.S.), Jerusalem, Israel. Additional support was provided by the Fund for the Promotion of Research at the Technion and by the Otto Meyerhof Center for Biotechnology, established by the Minerva Foundation (Munich, Germany). V.B. acknowledges the financial support by the Center of Absorption in Science, the Ministry of Immigration Absorption, and the Ministry of Science and Arts, Israel (Kamea Program).

* Corresponding authors. Y.S.: Department of Food Engineering and Biotechnology, Technion, Haifa 32000, Israel; tel, 972-4-8293072; fax, 972-4-8320742; e-mail, yshoham@tx.technion.ac.il. T.B.: Department of Chemistry, Technion, Haifa 32000, Israel; tel, 972-4-8292590; e-mail, chtimor@techunix.technion.ac.il.

‡ Department of Food Engineering and Biotechnology, Technion-Israel Institute of Technology.

§ Department of Chemistry, Technion-Israel Institute of Technology.

|| Department of Inorganic Chemistry and The Laboratory for Structural Chemistry and Biology, The Hebrew University of Jerusalem.

⊥ Architecture et Fonction des Macromolécules Biologiques, UMR6098, CNRS, and Universités d'Aix-Marseille I and II.

Institute of Catalysis Science and Technology, Technion-Israel Institute of Technology.

10.1021/bi034505o CCC: $25.00
Published on Web 08/13/2003

Scheme 1: Proposed Mechanistic Pathway for Retaining Glycosidases

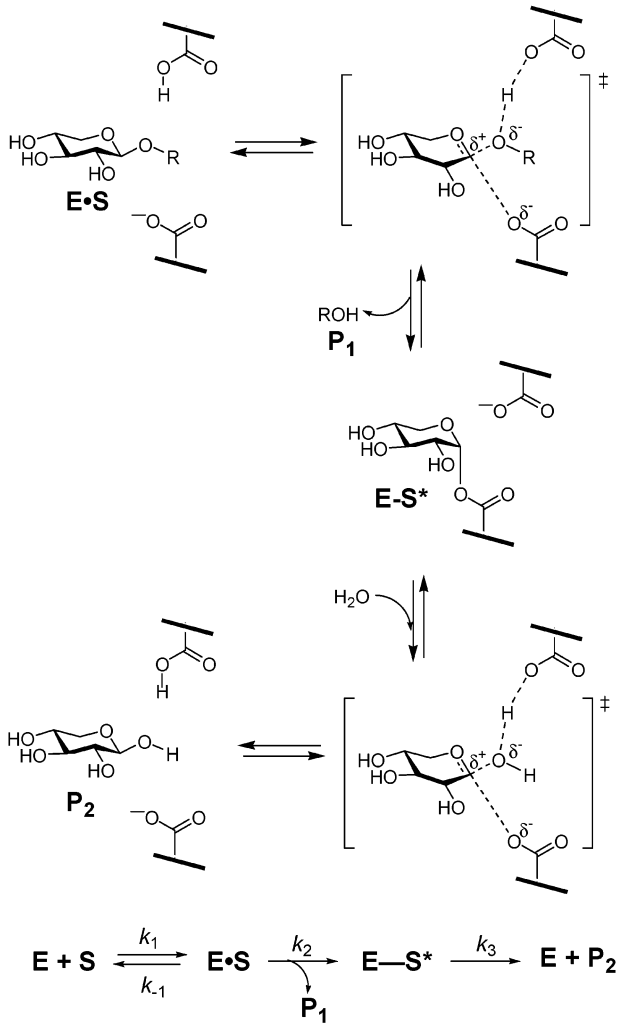

enzymes are capable of accelerating the hydrolysis of the glycosidic bond up to 10^{17}-fold, making them of the most proficient catalysts in nature. Hydrolysis of the glycosidic bond is carried out either by retention or by inversion of the anomeric configuration of the substrate. Inverting glycosidases use a single-displacement mechanism with the assistance of a general acid and a general base. Retaining glycosidases follow a two-step double-displacement mechanism as shown in Scheme 1, involving two key active site residues, one functioning as the nucleophile and the other as the acid−base (*8*).

On the basis of amino acid sequence similarities, glycoside hydrolases have been classified into more than 86 families that are constantly updated at the carbohydrate-active enzymes server (http://afmb.cnrs-mrs.fr/CAZY). β-D-Xylosidases are currently divided into families 3, 39, 43, 52, and 54 of glycoside hydrolases (*9*, *10*). While a large body of kinetic and mechanistic data has been collected for most of these families, very little is known regarding the catalytic mechanism of family 52. The enzymes of family 43 are probably the most studied β-D-xylosidases, and these were shown to cleave the glycosidic bond with an inversion of the anomeric configuration (*11*−*13*). Very recently, the three-dimensional structure of a member of this family was determined (*14*). Members of family 39, which were found to proceed via retention of the anomeric configuration (*15*), were also studied extensively, including the identification of their catalytic residues (*16*−*19*). Currently, only five enzymes of family 52 are known, none of which has been subjected to detailed kinetic analysis.

Previously, we reported the cloning and sequencing of a 23.5 kb chromosomal segment from *Geobacillus stearothermophilus* that contains a cluster of xylan utilization genes that includes an open reading frame of a β-xylosidase (*xynB2*) gene showing homology to family 52 glycoside hydrolases (*20*). The enzyme was subcloned and purified, and its stereochemical course of hydrolysis showed that the configuration of the anomeric carbon was retained, indicating that a retaining mechanism prevails in family 52 glycoside hydrolases (*21*). Enzymes belonging to the same family are believed to share common catalytic properties and three-dimensional structures. Since the β-xylosidase from *G. stearothermophilus* T-6 (XynB2) can be readily overexpressed and purified, it can serve as an excellent candidate for structure function studies and as a representative of family 52 glycoside hydrolases. This study describes the first detailed mechanistic study of a family 52 β-D-xylosidase, providing insights into substrate specificity, binding properties, rate-limiting steps, and possible transition state structures.

MATERIALS AND METHODS

Substrates. 4-Nitrophenyl β-D-xylopyranoside, 2-nitrophenyl β-D-xylopyranoside, 4-methylumbelliferyl β-D-xylopyranoside, glucose, isopropyl β-D-thioglucoside, δ-gluconolactone, 1-deoxynojirimycin, 1,6-anhydro-β-glucopyranose, and all of the 4-nitrophenyl glycosides were from Sigma Chemical Co. 4-Bromophenyl β-D-xylopyranoside, phenyl β-D-xylopyranoside, and 3,4-dimethylphenyl β-D-xylopyranoside were from Charlock Enterprises Ltd. (London, England). 2,5-Dinitrophenyl β-D-xylopyranoside, 3,4-dinitrophenyl β-D-xylopyranoside, 2,4,6-trichlorophenyl β-D-xylopyranoside, 3-nitrophenyl β-D-xylopyranoside, and 4-nitrophenyl β-D-xylobioside were synthesized as described by Ziser et al. (*22*). 4-Methoxyphenyl β-D-xylopyranoside was synthesized as follows. (Trimethylsilyl)trifluoromethanesulfonate (0.99 g, 0.004 mol) was added to a mixture of the tetraacetate of D-xylose (3.55 g, 0.011 mol) and 4-methoxyphenol (1.52 g, 0.012 mol) in dry dichloromethane (50 mL) at 0 °C. The reaction was carried out at 0 °C and monitored by TLC (CH_2Cl_2/EtOAc, 12:1). After 1.5 h the reaction mixture was diluted with EtOAc (150 mL) and neutralized with concentrated $NaHCO_3$ (2 × 30 mL), and the organic layer was washed with NaCl (2 × 50 mL), dried ($MgSO_4$), and concentrated. The residue was washed with anhydrous methanol (2 × 50 mL), concentrated, and dried under high vacuum conditions. A solution of 0.5 M NaOMe in methanol (7 mL) was added to the stirred solution of the residue that was obtained in anhydrous MeOH (40 mL) at 0 °C. The reaction was carried out at 0 °C and monitored by TLC (MeOH/$CHCl_3$, 1:6). After 2.5 h the reaction mixture was loaded on a silica gel column (100% MeOH), and fractions that contained the target product were combined and concentrated. The residue was purified by chromatography on a silica gel column (MeOH/$CHCl_3$, 1:9) to give the final compound (1.37 g, 48%). ^{1}H NMR data of this compound were in agreement with the literature (*18*). 2-Naphthyl β-D-xylopyranoside was prepared using the same procedure as

described for 4-methoxyphenyl β-D-xylopyranoside. A mixture of the tetraacetate of D-xylose (2.20 g, 0.007 mol) and 2-naphthol (1.09 g, 0.008 mol) in dry dichloromethane (50 mL) at 0 °C was treated with (trimethylsilyl)trifluoromethanesulfonate (0.62 g, 0.003 mol). Deprotection of the crude mixture was obtained with a solution of 0.5 M NaOMe in methanol (5 mL), and chromatography on a silica gel column ($MeOH/CHCl_3$, 1:9) of the crude mixture produced the pure target compound (0.82 g, 43%). ^1H NMR data of the compound were in agreement with the literature (*18*). 2,4-Dinitrophenyl β-D-xylopyranoside was a gift from Prof. Yaw-Kuen Li. The C-1 deuterated substrates, 2,5-dinitrophenyl β-D-xylopyranoside, 2-nitrophenyl β-D-xylopyranoside, and 2-acetamidophenyl β-D-xylopyranoside, were generous gifts from Dr. David Vocadlo and Prof. Stephen G. Withers. Xylooligosaccharides were purchased from MegaZyme Ltd. (Bray, Republic of Ireland).

Mutagenesis, Protein Expression, and Purification. The *xynB2* gene (GenBank accession number AJ305327) from *G. stearothermophilus* T-6 was cloned in the pET9d vector, overexpressed in *Escherichia coli* BL21(DE3), and purified as previously reported (*21*). Site-directed mutagenesis was performed using the QuikChange site-directed mutagenesis kit (Stratagene, La Jolla, CA). The mutagenic primers for the mutant gene (D495G) were as follows (the mutated nucleotides are in bold type): 5′-GGAAATCACAACGTA**C**G**GG**AGTTTGGATGTTTCTCTTGG-3′ and 5′-CCAAGAGAAACATCCAAACT**CC**C**G**TACGTTGTGATTTCC-3′. The mutagenic primer was designed to include the mutation and a restriction site that was used for screening the appropriate mutant. The mutated gene was sequenced to confirm that only the desired mutations were inserted, and the protein was overexpressed and purified as described for the wild type.

Kinetic Studies. Steady-state kinetic studies were performed by following the spectroscopic absorbance changes in the UV−visible range, using an Ultrospec 2100 pro spectrophotometer (Pharmacia) equipped with a temperature-stabilized water circulating bath. Initial hydrolysis rates were determined by incubating 500 μL of different substrate concentrations (ranging from 0.1 to 7 K_m where applicable) in 100 mM phosphate buffer (pH 7.0) containing 1 mg/mL BSA at 40 °C within the spectrophotometer until thermal equilibration was achieved. Reactions were initiated by the addition of 100 μL of appropriately diluted enzyme, and the release of the phenol-derived product was monitored at the appropriate wavelength. For highly reactive substrates, blank mixtures containing all of the reactants except the enzyme were used to correct for spontaneous hydrolysis of the substrates. The wavelength monitored and extinction coefficients used for each substrate were as follows: 2,4-dinitrophenyl, 400 nm, $\Delta\epsilon = 8.48\ mM^{-1}\ cm^{-1}$; 2,5-dinitrophenyl, 420 nm, $\Delta\epsilon = 3.68\ mM^{-1}\ cm^{-1}$; 3,4-dinitrophenyl, 400 nm, $\Delta\epsilon = 11.15\ mM^{-1}\ cm^{-1}$; 2,4,6-trichlorophenyl, 312 nm, $\Delta\epsilon = 3.97\ mM^{-1}\ cm^{-1}$; 4-nitrophenyl, 420 nm, $\Delta\epsilon = 7.61\ mM^{-1}\ cm^{-1}$; 2-nitrophenyl, 420 nm, $\Delta\epsilon = 1.91\ mM^{-1}\ cm^{-1}$; 4-methylumbelliferyl, 355 nm, $\Delta\epsilon = 2.87\ mM^{-1}\ cm^{-1}$; 3-nitrophenyl, 380 nm, $\Delta\epsilon = 0.455\ mM^{-1}\ cm^{-1}$; 4-bromophenyl, 289 nm, $\Delta\epsilon = 0.626\ mM^{-1}\ cm^{-1}$; 2-naphthyl, 330 nm, $\Delta\epsilon = 0.871\ mM^{-1}\ cm^{-1}$; 2-acetamidophenyl, 288 nm, $\Delta\epsilon = 0.495\ mM^{-1}\ cm^{-1}$; phenyl, 277 nm, $\Delta\epsilon = 0.863\ mM^{-1}\ cm^{-1}$; 4-methoxyphenyl, 296 nm, $\Delta\epsilon = 1.09\ mM^{-1}\ cm^{-1}$; 3,4-dimethylphenyl, 285 nm, $\Delta\epsilon = 0.90\ mM^{-1}\ cm^{-1}$. Values of K_m and k_{cat} were determined by nonlinear regression analysis using the program GraFit 5.0 (*23*). Reducing sugar assays were performed as described previously (*24*). Inhibition studies were performed at 40 °C in 100 mM phosphate buffer (pH 7.0) including 1 mg/mL BSA using 4-nitrophenyl β-D-glucopyranoside as a substrate. K_i values for all inhibitors were determined using four to five different inhibitor concentrations covering the K_i value wherein each inhibitor concentration was added to different substrate concentrations covering the K_m value. Solutions of δ-gluconolactone were prepared immediately before use.

Isotope effects were determined by measuring the ratio of hydrolysis rates for protio and deuterio substrates. For 2,5-DNPX[1] and *o*NPX, saturating conditions were obtained ($7-8K_m$), allowing the determination of the first-order rate constants (V_{max}). For *o*NHAcX, the second-order rate constant (V_{max}/K_m) was determined using low substrate concentration ($^1/_{18}K_m$). The isotope effect as determined is an average of seven to ten measurements.

pH dependence studies were carried at 40 °C with *p*NPX as a substrate. Mixtures containing 600 μL of 1 mg/mL BSA and different concentrations of substrate solutions in the appropriate buffer were prewarmed until the reaction was initiated by the addition of 200 μL of appropriately diluted enzyme. The buffers used were at a final concentration of 100 mM and were citric acid−Na_2HPO_4 (pH 3.5−6.5), phosphate buffer (pH 6.0−8.0), and Tris-HCl buffer (pH 7.5−8.5). The pH range employed in this study included only pH values for which the enzyme was stable for at least 5 min. Reactions were monitored continuously, and upon completion the actual pH was measured to verify that the pH has not changed. Extinction coefficients of 4-nitrophenol were determined at each pH, and values of K_m and k_{cat} were determined as described above. The pK_a values assigned to the ionizable groups were determined using the program GraFit 5.0.

Microcalorimetry Titration Studies. Titration calorimetry measurements were performed with a Microcal VP-ITC titration calorimeter (Microcal Inc., Northampton, MA) as described previously (*25*). Aliquots of 10 μL of the ligand solution at 8− 20 times the active site concentration were added via a 250 μL rotating stirrer−syringe to the cell solution containing 1.41 mL of 0.1−0.2 mM protein solution. All titrations were performed at 30 °C in 50 mM Tris-HCl (pH 7.0) buffer containing 100 mM NaCl and 0.02% azide. Ligand−protein titration curves were corrected for the heat of dilution by subtraction of the blank titration curves obtained by titration of buffer in the cell with the same ligand solution in the syringe. Calorimetric data were analyzed with the Origin 5.0 program (MicroCal).

RESULTS AND DISCUSSION

Recently, we described the cloning, expression, purification, and preliminary biochemical characterization of a glycoside hydrolase from family 52 (*20*, *21*). Members of this family were found to be β-xylosidases as previously

[1] Abbreviations: *p*NPX, 4-nitrophenyl β-D-xylopyranoside; *o*NPX, 2-nitrophenyl β-D-xylopyranoside; 2,5-DNPX, 2,5-dinitrophenyl β-D-xylopyranoside; *o*NHAcX, 2-acetamidophenyl β-D-xylopyranoside.

Table 1: Michaelis−Menten Parameters for the Hydrolysis of Aryl Glycosides by XynB2[a]

substrate	k_{cat} (s^{-1})	K_m (mM)	k_{cat}/K_m (s^{-1} mM^{-1})
4-nitrophenyl β-D-xylopyranoside	18	0.13	140
4-nitrophenyl β-D-glucopyranoside	0.26	12	0.022
4-nitrophenyl β-D-galactopyranoside	0.007	0.20	0.034
4-nitrophenyl β-D-fucopyranoside	0.006	0.49	0.013
4-nitrophenyl α-L-arabinopyranoside	∼4.6[b]	∼35	∼0.13
4-nitrophenyl α-L-arabinofuranoside	0.11	0.71	0.16
4-nitrophenyl β-D-glucuronide	0.068	0.23	0.30
4-nitrophenyl β-D-mannopyranoside	ND[c]		
4-nitrophenyl α-D-xylopyranoside	ND		

[a] Conditions: 100 mM phosphate buffer, pH 7.0, 40 °C. [b] Parameters were estimated due to the high K_m value and low substrate solubility. [c] Not detectable (less than 10^{-6}).

Scheme 2: Haworth Perspective Structures of 4-Nitrophenyl Glycosides Tested To Determine Substrate Specificity of XynB2

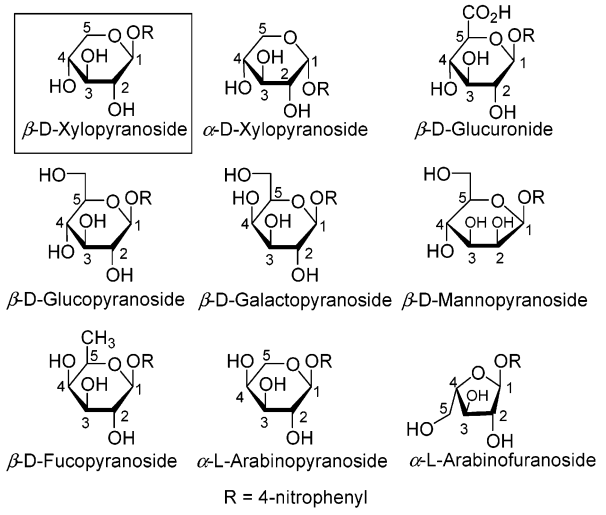

reported for the enzymes from *G. stearothermophilus* 21 (*26*), *G. stearothermophilus* 236 (*27*), and *Aeromonas caviae* ME-1 (*28*).

Substrate Specificity. Most glycoside hydrolases are highly specific with regard to the identity of the substrate glycone. According to the well-accepted nomenclature proposed previously (*29*), the glycone moiety occupies the −1 subsite in the enzyme active site, while the aglycon moiety occupies the +1 subsite. The specificity of XynB2 at the −1 subsite was evaluated by examining the rate constants for the hydrolysis of several 4-nitrophenyl glycoside substrates (Table 1, Scheme 2).

XynB2 significantly prefers substrates with xylose at the glycone moiety (k_{cat}/K_m = 140) and, as expected, has no detectable activity toward substrates with the opposite anomeric configuration such as 4-nitrophenyl α-D-xylopyranoside. The k_{cat} value for hydrolysis of the natural substrate xylobiose is 8 s^{-1}, as measured via the reducing sugar assay. Many xylosidases including members of families 3, 43, and 54 possess α-L-arabinofuranoside activity (*30*, *31*) while some α-L-arabinofuranosidases have β-D-xylosidase activity (*32*). This is probably the consequence of the spatial similarity of the hydroxyl groups and glycosidic bond orientations in β-D-xylopyranosides and α-L-arabinofuranosides (Scheme 2). As with other β-D-xylosidases, XynB2 also hydrolyzes 4-nitrophenyl α-L-arabinofuranoside (k_{cat} = 0.11 s^{-1}) although with very low catalytic efficiency (measured by relative k_{cat}/K_m values). Another family 52 β-xylosidase from *A. cavie* ME-1 also exhibited very low α-L-arabinofuranosidase activity (*28*). Interestingly, XynB2 also hydrolyzes 4-nitrophenyl α-L-arabinopyranoside. The latter has a pyranose ring structure similar to that of β-D-xylopyranoside and only differs by the configuration at the C4 hydroxyl (Scheme 2). Comparison of the kinetic parameters between α-L-arabinofuranoside and α-L-arabinopyranoside suggests that the orientation of the C4 hydroxyl group has more effect on substrate binding (K_m values of 0.71 and ∼35 mM, respectively; Table 1) than it has on bond cleavage (k_{cat} values of 0.11 and ∼4.6 s^{-1}, respectively), although the catalytic efficiency for both substrates is similar. Substitution of C5 with a hydroxymethylene group as in the glucopyranoside substrate substantially reduced the catalytic efficiency in terms of k_{cat}/K_m (0.022 s^{-1} mM^{-1}). When both C4 and C5 are substituted, as in β-D-galactopyranoside and β-D-fucopyranoside, the catalytic efficiency remains at the same low level as for the hydrolysis of 4-nitrophenyl β-D-glucopyranoside. Interestingly, the residual activity for hydrolysis of the glucoside sugar is totally abolished when the C2 hydroxyl group is axial as in the β-D-mannoside sugar. It was previously shown in other glycosidases that noncovalent interactions between the enzyme and the C2 hydroxyl contribute substantially (18−22 kJ mol^{-1}) to stabilization of the transition states (*33*). Surprisingly, the catalytic efficiency for the hydrolysis of 4-nitrophenyl β-D-glucuronide (k_{cat}/K_m = 0.3 s^{-1} mM^{-1}) is the highest among all other substrates tested (except of course for 4-nitrophenyl β-D-xylopyranoside). Since enzyme complementary to the transition state implies that k_{cat}/K_m is at a maximum, the interaction of XynB2 with the charged carboxylic group on C5 has probably some stabilizing effect on the transition states (*34*). Together, these results demonstrate the high specificity of XynB2 for xylose as the glycone moiety, consistent with the assignment of XynB2 as a β-D-xylosidase.

Substrate Binding. To further examine the ability of XynB2 to interact with xylooligosaccharides, we measured the binding properties of xylobiose and xylotriose to XynB2 by means of isothermal titration calorimetry (ITC). Using ITC, the enthalpy of binding (Δ*H*) and the equilibrium association constant (K_a), and thus the free energy of association (Δ*G*), can be determined in a single experiment (*35*). Since the wild-type enzyme hydrolyzes its substrates and subsequently releases them from its active site, the energetic parameters for binding could not be measured. Therefore, ITC experiments were performed with the acid−base catalytic mutant XynB2-D495G (*36*). Rates of hydrolysis by this mutant are 10^3-fold lower (for hydrolysis of 2,5-DNPX k_{cat} = 64 and 0.057 s^{-1} for XynB2 and XynB2-D495G, respectively). Calorimetric titration curves of the enzyme with xylobiose and xylotriose are shown in Figure 1, and the thermodynamic parameters are summarized in Table 2.

As shown in Table 2, the binding constant, K_B, of xylobiose (17.1×10^4 M^{-1}) is much larger than for xylotriose (9.6×10^4 M^{-1}), indicating that xylobiose binds more tightly in the active site than xylotriose. All of the binding reactions were enthalpically driven with little positive entropy value for xylotriose. The enthalpy for binding of xylobiose is higher

Table 2: Thermodynamic Parameters of Binding of Xylooligosaccharides to XynB2-D495G

xylo-oligomer	n	$K_B \times 10^4$ (M^{-1})	K_D (μM)	ΔH_B (kcal mol^{-1})	$T\Delta S_B$ (kcal mol^{-1})	ΔG_B (kcal mol^{-1})
X2	0.95	17.1 ± 0.3	5.9	-13.0 ± 0.1	-5.8	-7.2
X3	0.97	9.6 ± 0.7	10.4	-5.2 ± 0.2	1.7	-6.9

than for xylotriose, suggesting that the additional xylose unit disrupts to some extent the hydrogen bond network created upon substrate binding. For these xylooligomers, there was an excellent agreement to a single binding site as evidenced by the stoichiometry constant approaching the value of 1. Although xylotriose has lower affinity to the active site, it is still interesting to determine whether the three xylose units occupy subsites -2, -1, $+1$ or -1, $+1$, $+2$, with cleavage taking place between the -1 and $+1$ subsites. Since β-D-xylosidases are considered to be exoglycosidases removing one xylose unit from the nonreducing end of xylooligosaccharides, it is expected that xylotriose would occupy subsites -1, $+1$, and $+2$. This was initially tested by tracking the reaction products via thin-layer chromatography (TLC) for hydrolysis of 4-nitrophenyl β-D-xylobioside, with xylose and 4-nitrophenyl β-D-xyloside being the expected initial products. However, since strong transglycosylation occurred, only the release of 4-nitrophenyl β-D-xyloside ($R_f = 0.78$, EtOAc/MeOH/H_2O, 7:2:1) and higher xylooligosaccharides ($R_f = 0.48-0.62$) was observed without any xylose detected (TLC not shown). Transglycosylation reactions happen when the anomeric carbon of the enzyme−substrate intermediate is attacked by a hydroxyl group of another sugar in place of water, resulting in substrate polymerization. To prevent this occurrence, a high concentration of methanol (10 M) was added to the reaction mixture. Many retaining glycoside hydrolases have the ability to transfer glycosyl residues to low molecular weight alcohols. Thus, addition of alcohol to the reaction will result with the formation of the corresponding alkyl glycoside. Therefore, if XynB2 transfers the xylosyl residue to methanol, the initial products will supposedly be methyl β-D-xyloside and methyl β-D-xylobioside in the case of -1, $+1$, $+2$ and of -2, -1, $+1$ subsite occupation, respectively. Indeed, methyl β-D-xyloside ($R_f = 0.61$) was accumulated with time, and no methyl β-D-xylobioside was observed even at the very initial stages of hydrolysis. 4-Nitrophenyl β-D-xyloside, which is formed and rapidly hydrolyzed, was also observed (TLC not shown). These results suggest that XynB2 removes only one xylose unit from the nonreducing end of xylotriose, indicating that the substrate is preferentially occupied at subsites -1, $+1$, and $+2$. XynB2 is also capable of releasing xylose from birch wood xylan (results not shown), and this is in good accordance with β-D-xylosidases being true exo-oligosaccharidases, removing a monosacchraide unit from the nonreducing end of xylooligomers.

pH Dependence. A pH dependence activity profile of an enzyme can provide meaningful information about the key ionizable groups within its active site. The kinetic constants of XynB2 for hydrolysis of *p*NPX were determined at different pH values in the range of 3.5−8.5. The pH dependence profile of the enzyme presented in Figure 2 is a typical bell-shaped curve as observed for many other glycoside hydrolases (*37*−*39*).

This curve suggests that enzymatic catalysis depends on two ionizable amino acid residues. The pK_a values of these ionizable groups in the free enzyme were derived from the plot of k_{cat}/K_m versus pH and are 4.2 and 7.3 (Figure 2a). Likewise, the pK_a values in the enzyme−substrate complex were derived from the plot of k_{cat} versus pH and are <4 and 7.3 (Figure 2b). The lower pK_a in the enzyme−substrate complex could not be determined accurately as the enzyme was insoluble at low pH. Nonetheless, this pK_a value appears to be lower than the corresponding value in the free enzyme. Thus, enzymatic catalysis for both the free and the enzyme−substrate complex requires one group in its protonated form (higher pK_a) and the other in its deprotonated form (lower pK_a). Using NMR titration experiments, McIntosh et al. measured directly the pK_a values of the two carboxylic catalytic residues (the nucleophile and the acid−base) of *Geobacillus circulans* xylanase. The values obtained correlated well with those derived from the pH dependence profile (*40*). Accordingly, the pK_a values found for XynB2 also reflect the catalytic pair. The higher pK_a attributed to the acid−base catalyst is much higher than for a normal carboxylic residue, probably resulting from charge repulsion with the nearby (5 Å for retaining enzymes) charged proximal nucleophile. Interestingly, the lower pK_a assigned to the nucleophile is shifted downward upon binding of the substrate. This observation, found also for other glycosidases (*38*, *41*, *42*), is probably a consequence of changes occurring in the hydrogen bond network and/or by a less hydrophobic environment in the active site (*43*). Thus, binding of substrate results in lowering the pK_a assigned to the nucleophile, thereby making it more acidic. This pH dependence profile indicates that enzymatic catalysis depends on two ionizable residues within the active site, and these can be attributed to the acid−base and nucleophile residues.

Mechanism of Hydrolysis and Substrate Reactivity Studies. Glycoside hydrolases cleave the glycosidic bond either by retention or by inversion of the anomeric configuration of the substrate (*8*). Inverting glycosidases use a single-displacement mechanism with the assistance of a general acid and a general base. Catalysis by retaining glycoside hydrolases follows the mechanistic pathway shown in Scheme 1. This is a two-step double-displacement mechanism involving the formation and breakdown of a covalent enzyme-bound intermediate, E−S*. This intermediate was demonstrated in crystal structures for several retaining glycoside hydrolases by trapping the enzyme−sugar complex using fluorosugars (*44*). Very recently, it was elegantly shown by means of mass spectrometry and X-ray crystallography that the intermediate in the hen egg white lysozyme from family 22 is also a covalent enzyme-bound entity and not a long-lived ion pair as proposed earlier (*45*). The two chemical steps undertaken at the enzyme active site proceed through transition states with an oxocarbenium ion character and include the following: a glycosylation step, in which the enzyme's nucleophilic residue, usually Glu or Asp, is glycosylated with the sugar substrate; a deglycosylation step, in which the above glycosyl-enzyme intermediate undergoes hydrolysis to reconstitute free enzyme. During the glycosylation step, the enzymatic acid−base catalytic residue is assumed to protonate the glycosidic bond oxygen of the substrate, thereby facilitating bond cleavage by stabilizing the leaving group (P_1). During this event, the enzymatic nucleophile

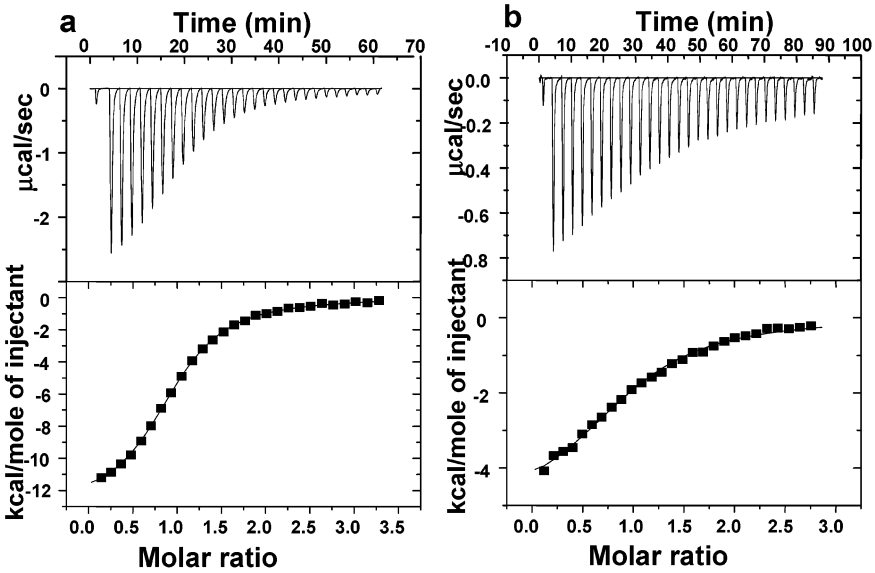

FIGURE 1: Calorimetric titration of XynB2 (catalytic mutant) with (a) xylobiose and (b) xylotriose. The top half of each experiment shows the raw data for calorimetric titration, and the lower half displays the integrated injection heats from the upper panel, corrected for control dilution heats. The solid line is the curve of best fit that was used to derive parameters n (stoichiometry), K_B, and ΔH.

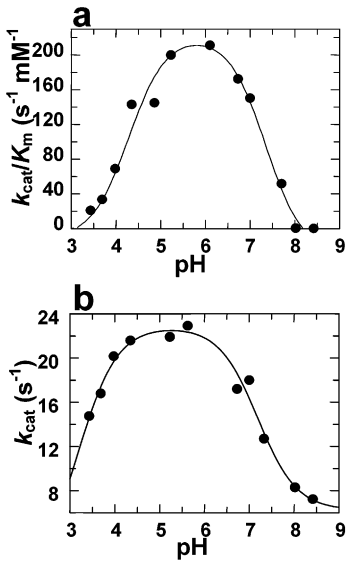

FIGURE 2: pH dependence of the kinetic parameters for the hydrolysis of 4-nitrophenyl β-D-xylopyranoside by XynB2. (a) Plot of k_{cat}/K_m versus pH. (b) Plot of k_{cat} versus pH.

attacks the anomeric carbon of the sugar substrate to form a covalent glycosyl-enzyme intermediate (E−S*). In the deglycosylation step, the carboxylate of the acid−base catalytic group serves as a general base to activate an incoming water molecule, which attacks the anomeric carbon of the sugar in the glycosyl-enzyme intermediate to form free sugar product (P_2) and reconstituted enzyme, and thus accomplishing the catalytic cycle.

We have previously shown, using NMR spectroscopy, that XynB2 of family 52 operates with an overall retention of the anomeric configuration and presumably follows a double-displacement mechanism as described above (*21*). The broad specificity for the aglycon moiety observed for many glycoside hydrolases, including XynB2, allowed us to determine the kinetic constants of the enzyme for hydrolysis of various aryl β-D-xylopyranoside substrates bearing different leaving groups with different pK_a values. The substrates used and the kinetic constants are summarized in Table 3, and the Brønsted plots for k_{cat} and k_{cat}/K_m are illustrated in Figure 3.

Table 3: Kinetic Parameters for Hydrolysis of Aryl β-D-Xylosides by XynB2[a]

aglycon	pK_a	k_{cat} (s^{-1})	K_m (mM)	k_{cat}/K_m (s^{-1} mM^{-1})
2,4-dinitrophenyl	3.96	63	0.24	260
2,5-dinitrophenyl	5.15	64	0.67	95
3,4-dinitrophenyl	5.36	50	0.15	335
2,4,6-trichlorophenyl	6.39	61	0.81	75
4-nitrophenyl	7.18	18	0.13	140
2-nitrophenyl	7.22	73	0.46	160
4-methylumbelliferyl	7.53	80	0.35	230
3-nitrophenyl	8.39	41	0.87	47
4-bromophenyl	9.34	13	0.63	21
2-naphthyl	9.51	21	1.4	15
2-acetamidophenyl	9.96	3.1	1.8	1.7
phenyl	9.99	15	4.4	3.4
4-methoxyphenyl	10.20	13	2.3	5.8
3,4-dimethylphenyl	10.32	12	3.9	3.0

[a] Conditions: 100 mM phosphate buffer, pH 7.0, 40 °C.

The Brønsted plot of log k_{cat} versus the aglycon pK_a values shown in Figure 3a reveals a biphasic relationship as observed for many other retaining glycoside hydrolases from different families (*37*, *46*−*48*), including the family 39 β-xylosidase from *Thermoanaerobacterium saccharolyticum* (*18*). Interestingly, no such behavior was observed for the β-xylosidase from *Trichoderma koningii* G-39 (unknown classification) (*49*). The biphasic nature of the Brønsted plot provides good confirmation for a two-step mechanism, and its shape is best understood upon examination of the catalytic constant k_{cat}. In a double-displacement mechanism involving an enzyme−substrate intermediate, $k_{cat} = k_2k_3/(k_2 + k_3)$, and k_2 and k_3 are the first-order rate constants of the glycosylation and deglycosylation step, respectively. Thus, when either rate constant is much larger than the other, k_{cat} will approach the value of the rate-limiting rate constant (e.g., if $k_2 \gg k_3$, then $k_{cat} \approx k_3$, and if $k_2 \ll k_3$, then $k_{cat} \approx k_2$). In addition, since the second step (deglycosylation) proceeds through hydrolysis of the same xylosyl-enzyme intermediate, regardless of the substrate reactivity, the same overall rate would

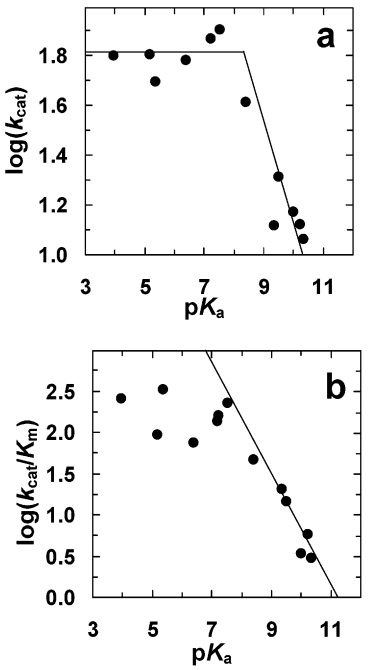

FIGURE 3: Brønsted plots relating turnover numbers and catalytic efficiencies of XynB2 with the leaving group ability of the substituted phenols. (a) Plot of log k_{cat} versus pK_a of the aglycon. (b) Plot of log(k_{cat}/K_m) versus pK_a of the aglycon.

be observed if this step is rate limiting, and thus k_{cat} will be invariant for hydrolysis of all substrates for which the second step is rate limiting. Conversely, since the first step (glycosylation) involves protonation of the leaving group, the rate of this step strongly depends on the leaving group ability, which is reflected by its pK_a. Therefore, if this step is rate limiting, k_{cat} will vary with substrate reactivity. Taking the above into account together with the Brønsted plot (Figure 3a) for XynB2, it is evident that glycosylation is the rate-limiting step for hydrolysis of substrates with poor leaving groups (pK_a > 8, k_{cat} values vary with substrate reactivity) and deglycosylation for hydrolysis of substrates with good leaving groups (pK_a < 8, k_{cat} values are invariant). A strong indication for the deglycosylation step being rate limiting (for good substrates) is the acceleration of the reaction rate upon addition of external nucleophiles such as dithiothreitol (*18*, *46*, *49*) or even azide (*19*) to the reaction mixture. In some cases, these anions compete effectively with the incoming water in the deglycosylation step to attack the anomeric carbon of the substrate in the covalent intermediate, thereby accelerating the rate of this step. If indeed the deglycosylation step is rate limiting, k_{cat} values should increase upon increasing concentrations of the external nucleophile. However, no such rate enhancement was observed for the hydrolysis of 2,5-DNPX (a substrate for which deglycosylation is rate limiting) with XynB2 in the presence of dithiothreitol or azide up to a concentration of 1 M. Seemingly, the architecture of the XynB2 active site is such that it prevents these nucleophiles from entering and competing with the attacking water.

A Brønsted plot of log(k_{cat}/K_m) against the pK_a value of the phenol leaving group is plotted in Figure 3b. For the two-step mechanism $k_{cat}/K_m = k_1k_2/(k_{-1} + k_2)$ and k_1 and k_{-1} are the rate constants for the Michaelis substrate−enzyme complex association and deassociation, respectively. Thus, the second-order rate constant, k_{cat}/K_m, is composed of rate constants along the reaction pathway from the free enzyme up to the first chemical step of bond cleavage (glycosylation). While k_{cat} governs the glycosylation step only for substrates with pK_a > 8, k_{cat}/K_m reflects this step for any substrate tested, regardless of its reactivity. Therefore, it would be best to probe the glycosylation step with respect to bond cleavage degree from a plot of log(k_{cat}/K_m) versus pK_a relationship. Despite the above, the Brønsted plot of log(k_{cat}/K_m) versus pK_a is also biphasic, as was also observed for other retaining glycoside hydrolases including the β-xylosidase from *T. saccharolyticum* (*18*) and the β-glucosidases from *Agrobacterium faecalis* (*46*), *Streptomyces* species (*37*), and sweet almonds (*50*). This biphasic behavior could not be a consequence of a change of the rate-limiting step from glycosylation for poor substrates to deglycosylation for more reactive substrates since k_{cat}/K_m is independent of the deglycosylation step. Instead, it is possible that the biphasic nature might reflect a change in the enzyme−substrate association constant (k_1), which becomes the rate-limiting step for the highly reactive substrates. Alternatively, k_{cat}/K_m might not reflect only the glycosylation step for the highly reactive substrates, as this step becomes reversible. This was rationalized on the basis of previous observations showing that the low pK_a phenols are strong inhibitors and, as a result, may promote the reverse reaction generating back the aryl xyloside substrate, as suggested elsewhere (*18*). Therefore, the correlation of log(k_{cat}/K_m) with pK_a values was derived only for the poorer substrates. Indeed, the plot in Figure 3b reveals a considerable correlation between the pK_a and log(k_{cat}/K_m) for the poorer substrates with a slope of $\beta_{1g} = -0.82$. The large value of β_{1g} suggests a high amount of negative charge on the oxygen anion of the leaving group at the glycosylation transition state, resulting from substantial bond cleavage and/or relatively little proton donation by the acid−base catalyst. Collectively, these results are in good agreement with a two-step mechanism involving the formation and breakdown of an enzyme−substrate intermediate.

Table 4: Secondary Deuterium Kinetic Isotope Effects Measured with XynB2

substrate	pK_a	rate-limiting step	k_H/k_D
[1-^{2}H]-2,5-DNPX	5.15	deglycosylation	1.06 ± 0.02
[1-^{2}H]-*o*NPX	7.22	deglycosylation	1.05 ± 0.02
[1-^{2}H]-*o*NHAcX	9.96	glycosylation	1.03 ± 0.02

Secondary Isotope Effect. The secondary α-deuterium kinetic isotope effect can be useful to distinguish between S_N1 and S_N2 reactions and may provide insights about the amount of oxocarbenium ion character developed at the transition states. An oxocarbenium ion is formed when the hybridization state of the C-1 atom changes from sp^3 to sp^2, a change that will be reflected by a pronounced isotope effect as measured through k_H/k_D. Typical expected values are in the range of $k_H/k_D \approx 1.2$ for complete S_N1 reaction type (provided that the C−O bond cleavage step is rate limitng) and $k_H/k_D \approx 1.0$ for complete S_N2 reaction type (*51*, *52*). The isotope effect for XynB2 using three different substrates with different pK_a values is presented in Table 4.

On the basis of the pK_a of the leaving group and the Brønsted plot (Figure 3a) it is likely that the rate-limiting step for hydrolysis of *o*-nitrophenyl β-D-xylopyranoside (pK_a = 7.22) and 2,5-dinitrophenyl β-D-xylopyranoside (pK_a = 5.15) is deglycosylation, while for *o*-acetamidophenyl

Table 5: Inhibition Constants for XynB2

inhibitor	K_i (mM)	K_m (mM)
glucose	130	
isopropyl β-D-thioglucoside	240	
δ-gluconolactone	8	
1-deoxynojirimycin	0.12	
1,6-anhydro-β-glucopyranose	580	
4-nitophenyl β-D-glucopyranose		12

β-D-xylopyranoside (pK_a = 9.96) glycosylation is rate limiting. Therefore, measuring the secondary α-deuterium kinetic isotope effect for these substrates gives an indication about the amount of oxocarbenium ion developed at the transition states of both the glycosylation and deglycosylation steps. The k_H/k_D values measured for both the glycosylation and the deglycosylation steps are relatively low, indicating little oxocarbenium ion character at the transition states. Many glycosidases, including the *T. saccharolyticum* β-xylosidase from family 39, exhibited higher values of k_H/k_D for the deglycosylation step, usually in the range of 1.08−1.25 (*18*, *46*, *53*, *54*). However, in some cases low k_H/k_D values were reported, for example, for the β-xylosidase from *T. koningii* G-39 (k_H/k_D = 1.02) (*49*), for the *E. coli* β-galactosidase, and for the β-glucosidases from almond and *Flavobacterium meningosepticum* (*48*, *53*, *55*). Several explanations may account for the low k_H/k_D values. First, the reaction may proceed by a concerted reaction mechanism, in which the nucleophile and the leaving group are tightly bound to the anomeric carbon. This, however, will have the effect of increasing the bending frequency for the anomeric hydrogen representing a very different transition state structure from the nonenzymatic reaction. Second, the enzymatic reaction may involve a complex reaction pathway that can greatly influence the magnitude of observed isotope effects for enzymes. For instance, it is possible that some other steps such as substrate binding and/or product release are partly rate determining and not the C−O bond cleavage (*52*, *53*, *56*). Third, interactions between the anomeric hydrogen and the enzyme at the reaction transition state may strengthen the C−H bending mode. This has been proposed previously to explain the observation of isotope effects at sites distant from the reaction center (*57*).

Inhibitor Studies. Inhibition studies are a valuable tool for exploring the enzymatic binding properties along the reaction coordinate. These studies can shed light on the substrate structures adopted at the ground state and transition state during catalysis. Since XynB2 has low, yet sufficient, activity toward 4-nitrophenyl β-D-glucopyranose, its inhibition constants toward several gluco derivative inhibitors could be measured.

All the compounds listed in Table 5 were found to inhibit XynB2 in a competitive manner. Ground state analogues with a chair conformation, such as glucose and isopropyl β-D-thioglucoside, bind with very low affinities to the enzyme with K_i over 100 mM. Even lower affinity is observed for 1,6-anhydro-β-glucopyranose, an analogue with a boat conformation (K_i = 580 mM). However, 1-deoxynojirimycin is a very potent inhibitor for XynB2 (K_i = 0.12 mM) as for many glycosidases (*58*). The charged ring nitrogen of this compound resembles the positive charge on the ring oxygen of the proposed oxocarbenium ion transition state. Thus, the strong inhibition is probably a result of the interaction between the enzyme and the positive charge character on the ring nitrogen (*59*). δ-Gluconolactone, which is a potent inhibitor for several glycosidases, binds with moderate affinity to XynB2. The half-chair conformation of this inhibitor mimics the partly planar conformation of the glycopyranosyl ring at the transition state because of its sp^2-hybridized anomeric center. Another β-xylosidase from *T. koningii* G-39 of unknown classification was also moderately inhibited by δ-xylonolactone (*49*), and the β-glucosidase from sweet almond was inhibited about 10-fold more strongly by 1-deoxynojirimycin than by δ-gluconolactone (*60*). It is still unclear what factor, shape or charge, is more important for glycosidase inhibition (*61*). Recent structural studies of enzyme−substrate complexes suggest that glycoside hydrolases can utilize different transition state and intermediate structures. For example, two family 11 xylanases display a $^{2,5}B$ boat conformation at the covalent glycosyl-enzyme intermediate, suggesting that a similar conformation is also adopted at the transition state (*62*, *63*), unlike the half-chair transition state presumably adopted by other glycosidases (*64*). Despite the absence of any structural information regarding XynB2, it is not unreasonable to speculate that the moderate affinity of the enzyme to the half-chair δ-gluconolactone analogue is a consequence of the different conformations of the inhibitor and the real transition state shape. In summary, inhibitors that mimic the proposed transition state structure bind with much higher affinity to XynB2 than ground state inhibitors.

In conclusion, the substrate specificity for the glycone moiety of XynB2 is considerably restricted to xylose. Binding of xylobiose and xylotriose is enthalpy driven with xylobiose binding more tightly than xylotriose to the active site. Enzymatic catalysis depends on two ionizable amino acid residues attributed to the acid−base and nucleophile. The Brønsted plot relationship is consistent with a double-displacement mechanism as expected for retaining enzymes, involving formation and breakdown of an enzyme−substrate intermediate. Bond cleavage is rate limiting for hydrolysis of substrates with poor leaving groups (pK_a > 8), whereas breakdown of the xylosyl-enzyme intermediate is rate limiting for hydrolysis of substrates with good leaving groups (pK_a < 8). Both transition states proceed with relatively low oxocarbenium ion character, indicating considerable pre-association of the catalytic nucleuophile and water in the glycosylation and deglycosylation steps, respectively. The results presented in this work are, to the best of our knowledge, the first detailed kinetic study performed on family 52 β-xylosidase.

ACKNOWLEDGMENT

We thank Dr. D. Vocadlo and Prof. S. G. Withers for kindly providing the deuterated aryl β-D-xylopyranoside substrates and Prof. Y. K. Li for generously providing 2,4-dinitrophenyl β-D-xylopyranoside.

REFERENCES

1. Beg, Q. K., Kapoor, M., Mahajan, L., and Hoondal, G. S. (2001) *Appl. Microbiol. Biotechnol. 56*, 326−338.
2. Suurnakki, A., Tenkanen, M., Buchert, J., and Viikari, L. (1997) *Adv. Biochem. Eng. Biotechnol. 57*, 261−287.
3. Galbe, M., and Zacchi, G. (2002) *Appl. Microbiol. Biotechnol. 59*, 618−628.

4. Mielenz, J. R. (2001) *Curr. Opin. Microbiol. 4*, 324−329.
5. Mackenzie, L. F., Wang, Q., Warren, R. A., and Withers, S. G. (1998) *J. Am. Chem. Soc. 120*, 5583−5584.
6. Jahn, M., Marles, J., Warren, R. A., and Withers, S. G. (2003) *Angew. Chem., Int. Ed. Engl. 42*, 352−354.
7. Wolfenden, R., Lu, X., and Young, G. (1998) *J. Am. Chem. Soc. 120*, 6814−6815.
8. Davies, G., Sinnott, M. L., and Withers, S. G. (1998) in *Comprehensive Biological Catalysis* (Sinnott, M. L., Ed.) Vol. 1, pp 119−209, Academic Press Ltd., London.
9. Henrissat, B., and Bairoch, A. (1996) *Biochem. J. 316*, 695−696.
10. Henrissat, B., and Davies, G. (1997) *Curr. Opin. Struct. Biol. 7*, 637−644.
11. Braun, C., Meinke, A., Ziser, L., and Withers, S. G. (1993) *Anal. Biochem. 212*, 259−262.
12. Padmaperuma, B., and Sinnott, M. L. (1993) *Carbohydr. Res. 250*, 79−86.
13. Kasumi, T., Tsumuraya, Y., Brewer, C. F., Kersters-Hilderson, H., Claeyssens, M., and Hehre, E. J. (1987) *Biochemistry 26*, 3010−3016.
14. Nurizzo, D., Turkenburg, J. P., Charnock, S. J., Roberts, S. M., Dodson, E. J., McKie, V. A., Taylor, E. J., Gilbert, H. J., and Davies, G. J. (2002) *Nat. Struct. Biol. 9*, 665−668.
15. Armand, S., Vieille, C., Gey, C., Heyraud, A., Zeikus, J. G., and Henrissat, B. (1996) *Eur. J. Biochem. 236*, 706−713.
16. Bravman, T., Mechaly, A., Shulami, S., Belakhov, V., Baasov, T., Shoham, G., and Shoham, Y. (2001) *FEBS Lett. 495*, 115−119.
17. Vocadlo, D. J., MacKenzie, L. F., He, S., Zeikus, G. J., and Withers, S. G. (1998) *Biochem. J. 335*, 449−455.
18. Vocadlo, D. J., Wicki, J., Rupitz, K., and Withers, S. G. (2002) *Biochemistry 41*, 9727−9735.
19. Vocadlo, D. J., Wicki, J., Rupitz, K., and Withers, S. G. (2002) *Biochemistry 41*, 9736−9746.
20. Shulami, S., Gat, O., Sonenshein, A. L., and Shoham, Y. (1999) *J. Bacteriol. 181*, 3695−3704.
21. Bravman, T., Zolotnitsky, G., Shulami, S., Belakhov, V., Solomon, D., Baasov, T., Shoham, G., and Shoham, Y. (2001) *FEBS Lett. 495*, 39−43.
22. Ziser, L., Setyawati, I., and Withers, S. G. (1995) *Carbohydr. Res. 274*, 137−153.
23. Leatherbarrow, R. J. (2001) Erithacus Software Ltd., Horley, U.K.
24. Garcia, E., Johnston, D., Whitaker, J. R., and Shoemaker, S. P. (1993) *J. Food Biochem. 17*, 135−145.
25. Wiseman, T., Williston, S., Brandts, J. F., and Lin, L. N. (1989) *Anal. Biochem. 179*, 131−137.
26. Baba, T., Shinke, R., and Nanmori, T. (1994) *Appl. Environ. Microbiol. 60*, 2252−2268.
27. Oh, H., and Choi, Y. (1994) *Korean J. Appl. Microbiol. Biotechnol. 22*, 134−142.
28. Suzuki, T., Kitagawa, E., Sakakibara, F., Ibata, K., Usui, K., and Kawai, K. (2001) *Biosci. Biotechnol. Biochem. 65*, 487−494.
29. Davies, G. J., Wilson, K. S., and Henrissat, B. (1997) *Biochem. J. 321*, 557−559.
30. Lee, R. C., Hrmova, M., Burton, R. A., Lahnstein, J., and Fincher, G. B. (2003) *J. Biol. Chem. 278*, 5377−5387.
31. Utt, E. A., Eddy, C. K., Keshav, K. F., and Ingram, L. O. (1991) *Appl. Environ. Microbiol. 57*, 1227−1234.
32. Shallom, D., Belakhov, V., Solomon, D., Gilead-Gropper, S., Baasov, T., Shoham, G., and Shoham, Y. (2002) *FEBS Lett. 514*, 163−167.
33. Zechel, D. L., and Withers, S. G. (1999) *Acc. Chem. Res. 33*, 11−18.
34. Fersht, A. (1999) *Structure and Mechanism in Protein Science*, 3rd ed., W. H. Freeman, New York.
35. Doyle, M. L. (1997) *Curr. Opin. Biotechnol. 8*, 31−35.
36. Bravman, T., Belakhov, V., Solomon, D., Shoham, G., Henrissat, B., Baasov, T., and Shoham, Y. (2003) *J. Biol. Chem. 278*, 26742−26749.
37. Vallmitjana, M., Ferrer-Navarro, M., Planell, R., Abel, M., Ausin, C., Querol, E., Planas, A., and Perez-Pons, J. A. (2001) *Biochemistry 40*, 5975−5982.
38. Malet, C., and Planas, A. (1997) *Biochemistry 36*, 13838−13848.
39. Moracci, M., Capalbo, L., Ciaramella, M., and Rossi, M. (1996) *Protein Eng. 9*, 1191−1195.
40. McIntosh, L. P., Hand, G., Johnson, P. E., Joshi, M. D., Korner, M., Plesniak, L. A., Ziser, L., Wakarchuk, W. W., and Withers, S. G. (1996) *Biochemistry 35*, 9958−9966.
41. Gomez, M., Isorna, P., Rojo, M., and Estrada, P. (2001) *Biochimie 83*, 961−967.
42. Keresztessy, Z., Kiss, L., and Hughes, M. A. (1994) *Arch. Biochem. Biophys. 314*, 142−152.
43. Inoue, M., Yamada, H., Yasukochi, T., Kuroki, R., Miki, T., Horiuchi, T., and Imoto, T. (1992) *Biochemistry 31*, 5545−5553.
44. Withers, S. G. (2001) *Carbohydr. Polym. 44*, 325−337.
45. Vocadlo, D. J., Davies, G. J., Laine, R., and Withers, S. G. (2001) *Nature 412*, 835−838.
46. Kempton, J. B., and Withers, S. G. (1992) *Biochemistry 31*, 9961−9969.
47. Bauer, M. W., and Kelly, R. M. (1998) *Biochemistry 37*, 17170−17178.
48. Li, Y. K., Chir, J., and Chen, F. Y. (2001) *Biochem. J. 355*, 835−840.
49. Li, Y. K., Yao, H. J., and Pan, I. H. (2000) *J. Biochem. (Tokyo) 127*, 315−320.
50. Dale, M. P., Kopfler, W. P., Chait, I., and Byers, L. D. (1986) *Biochemistry 25*, 2522−2529.
51. Sinnott, M. L., Garner, C. D., First, E., and Davies, G. (1998) in *Comprehensive Biological Catalysis* (Sinnott, M. L., Ed.) Vol. 4, pp 47−58, Academic Press Ltd., London.
52. Purich, D. L., and Allison, R. D. (2000) *Handbook of Biochemical Kinetics*, Academic Press Ltd., London.
53. Sinnott, M. L., and Souchard, I. J. (1973) *Biochem. J. 133*, 89−98.
54. Tull, C., and Withers, S. G. (1994) *Biochemistry 33*, 6363−6370.
55. Dahlquist, F. W., Rand-Meir, T., and Raftery, M. A. (1969) *Biochemistry 8*, 4214−4221.
56. Selwood, T., and Sinnott, M. L. (1990) *Biochem. J. 268*, 317−323.
57. Horenstein, B. A., Parkin, D. W., Estupinan, B., and Schramm, V. L. (1991) *Biochemistry 30*, 10788−10795.
58. Legler, G. (1990) *Adv. Carbohydr. Chem. Biochem. 48*, 319−384.
59. Kajimoto, T., Liu, K. K. C., Pederson, R. L., Zhong, Z. Y., Ichikawa, Y., Porco, J. A., and Wong, C. H. (1991) *J. Am. Chem. Soc. 113*, 6187−6196.
60. Dale, M. P., Ensley, H. E., Kern, K., Sastry, K. A., and Byers, L. D. (1985) *Biochemistry 24*, 3530−3539.
61. Heightman, T. D., and Vasella, A. T. (1999) *Angew. Chem., Int. Ed. Engl. 38*, 750−770.
62. Sidhu, G., Withers, S. G., Nguyen, N. T., McIntosh, L. P., Ziser, L., and Brayer, G. D. (1999) *Biochemistry 38*, 5346−5354.
63. Sabini, E., Sulzenbacher, G., Dauter, M., Dauter, Z., Jorgensen, P. L., Schulein, M., Dupont, C., Davies, G. J., and Wilson, K. S. (1999) *Chem. Biol. 6*, 483−492.
64. Rye, C. S., and Withers, S. G. (2000) *Curr. Opin. Chem. Biol. 4*, 573−580.

BI034505O